

# Design and implementation of fractional PID controller for rotary inverted pendulum

Chunyang Wang, Xu Liu, Hongwei Shi\*, Ruihao Xin, Xiang Xu

College of Electronic Information Engineering, Changchun University of Science and Technology, Changchun, 130022

E-mail: wangchunyang19@163.com

**Abstract:** As for the stability control problem for rotary inverted pendulum, the two closed-loop fractional order PID control scheme is used to control the pendulum. First, the mathematical model of rotary inverted pendulum is established according to the Euler-Lagrange equation. Then, a fractional order PID controller is designed based on the Bode ideal transfer function. Finally, the fractional order PID (FOPID) controller, fractional PD (FOPD) controller and integer order PD (IOPD) controller are applied to the rotary inverted pendulum system which based on the Quanser company loop simulation experiment platform. The results show that the FOPID controller is better than the FOPD and IOPD controller in stabilizing the system and the angle of the pendulum is closest to the stable equilibrium point.

**Key Words:** rotary inverted pendulum; fractional PID controller; Bode ideal transfer function; stable control

## 1 INTRODUCTION

The rotary inverted pendulum system is a nonlinear natural unstable system, and it is an ideal model to verify the control theory. At present, the control methods for rotary inverted pendulum mainly include PID control<sup>[1]</sup>, state feedback regulation<sup>[2]</sup>, linear two degree regulator (LQR)<sup>[3]</sup> and fuzzy control<sup>[4]</sup> etc. Among them, PID control is the most widely used in rotary inverted pendulum control. However, there are some defects in the PID method, such as poor stability and low robustness. In this regard, this paper introduces the calibration method of FOPID controller. The theory of fractional calculus has been established for more than 300 years, fractional calculus is the order of differentials and integrals, which can be any number or fraction, and the commonly used integer order calculus is a special form of fractional order. The fractional order controller is the extension of the traditional integer PID controller. It has two adjustable parameters over the integer PID controller, that is the order of integration  $\lambda$  and the order of differentiation  $\mu$ . It also has more than two degrees of freedom in design, which can achieve better control effect than IOPID controller. The traditional design methods for FOPID controller is only to stable system, such as Chen Yangquan<sup>[5]</sup> proposed the robust fractional order controller design method, this method is only applicable to the stable system, unstable system is not suitable for this method. This paper presents the Bode ideal transfer function method to design the FOPID controller, this method can solve the traditional fractional parameter tuning method is only for stable system design defects. This design method of FOPID controller can apply to unstable system, and the inverted pendulum system is the representative of the unstable system, and the experimental verification was

carried out on the rotary inverted pendulum of Quanser company. It provides a new reference idea for the design of fractional order controller.

## 2 MODELING OF ROTARY INVERTED PENDULUM SYSTEM

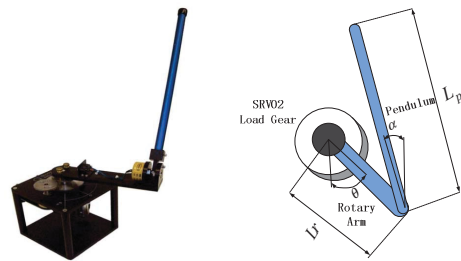


Fig.1 Rotary Inverted pendulum model

The Quanser Inverted Pendulum experiment is made up of a mechanical and an electrical subsystem<sup>[6]</sup>. The Quanser experimental set-up contains the following components: Quanser Q2-USB data acquisition board, The Power Amplifier, Quanser Pendulum Module, Quanser SRV02 servo Motor, PC equipped with Matlab/Simulink and Quarc software and two encoders.

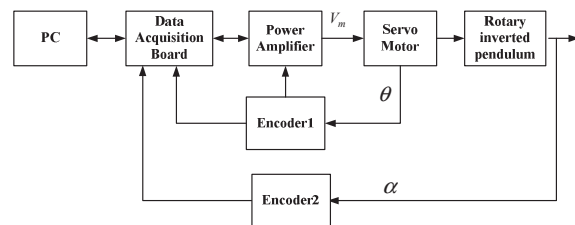


Fig.2 The structure diagram of the rotary inverted pendulum control system

Corresponding author: Hongwei Shi

This work is supported by Basic Research Program of Jilin Provincial Science & Technology Department(20130102025JC)

Table1. Actual System Parameter Of Rotary Inverted Pendulum

Parameter	Description	Value
$m_p$	Mass of Pendulum	0.127Kg
$L_p$	Pendulum length	0.3365m
$l_p$	Pendulum center of mass	0.1556m
$J_p$	The moment of inertia of pendulum about $\alpha$	1.1983e-3kg.m <sup>2</sup>
$B_p$	Viscous friction in pendulum rod joint	0.0024N.m.s/rad
$B_r$	Viscous friction in arm joint	0.0024N.m.s/rad
$L_r$	Arm length	0.216m
$l_r$	Arm center of mass	0.0619m
$J_r$	Moment of inertia about $\theta$	9.98e-4kg.m <sup>2</sup>
$m_r$	Mass of arm	0.257kg
$R_m$	Armature resistance	2.6 $\Omega$
$K_g$	SRV02 system gear ratio	70
$K_m$	Back-emf constant	0.007677
$K_t$	Motor torque constant	0.007682
$\eta_g$	Gear box efficiency	0.9
$\eta_m$	Motor efficiency	0.69
$g$	Gravitational acceleration	9.81m/s <sup>2</sup>

For the modeling of rotary inverted pendulum, the Euler-Lagrange equation modeling method is used in this paper. The motion equations of the angle of the rotary arm  $\theta$  and the angle of the pendulum  $\alpha$  relative to the voltage  $V_m$  of the servo motor are described:

$$\frac{\partial^2 L}{\partial t \partial \dot{q}_i} - \frac{\partial L}{\partial q_i} = Q_i \quad (1)$$

The variable  $q_i$  is called the generalized coordinate, which can be expressed as:

$$q(t)^T = [\theta(t) \ \alpha(t)] \quad (2)$$

The corresponding derivative is:

$$\dot{q}(t)^T = \left[ \frac{\partial \theta(t)}{\partial t} \ \frac{\partial \alpha(t)}{\partial t} \right] \quad (3)$$

The Euler-Lagrange equation based on the rotary inverted pendulum system is as follows:

$$\frac{\partial^2 L}{\partial t \partial \dot{\theta}} - \frac{\partial L}{\partial \theta} = Q_1 \quad (4)$$

$$\frac{\partial^2 L}{\partial t \partial \dot{\alpha}} - \frac{\partial L}{\partial \alpha} = Q_2 \quad (5)$$

$L$  is a Lagrange operator, which can be described as:

$$L = T - V \quad (6)$$

Among them, the  $T$  represents the total kinetic energy, and the  $V$  represents the potential energy, and the generalized force  $Q_i$  is used to describe the non-conservative forces (such as friction):

The generalized force on the rotary arm can be expressed as:

$$Q_1 = \tau - B_r \dot{\theta} \quad (7)$$

$\tau$  is a servo motor to control the torque produced by the rotary arm:

$$\tau = \frac{\eta_m \eta_g K_t K_g (V_m - K_g K_m \dot{\theta})}{R_m} \quad (8)$$

The generalized force on the pendulum can be expressed as:

$$Q_2 = -B_p \dot{\alpha} \quad (9)$$

After calculating  $T$ ,  $V$ ,  $L$  is obtained and two nonlinear equations of motion of rotary inverted pendulum can be obtained into the Euler-Lagrange equation as [7]:

$$\left( m_p L_r^2 + \frac{1}{4} m_p L_p^2 - \frac{1}{4} m_p L_p^2 \cos(\alpha)^2 + J_r \right) \ddot{\theta} - \left( \frac{1}{2} m_p L_p L_r \cos(\alpha) \right) \ddot{\alpha} + \left( \frac{1}{2} m_p L_p^2 \sin(\alpha) \cos(\alpha) \right) \dot{\theta} \dot{\alpha} + \left( \frac{1}{2} m_p L_p L_r \sin(\alpha) \right) \dot{\alpha}^2 = \tau - B_r \dot{\theta} \quad (10)$$

$$- \frac{1}{2} m_p L_p L_r \cos(\alpha) \ddot{\theta} + \left( J_p + \frac{1}{4} m_p L_p^2 \right) \ddot{\alpha} - \frac{1}{4} m_p L_p^2 \cos(\alpha) \sin(\alpha) \dot{\theta}^2 - \frac{1}{2} m_p L_p g \sin(\alpha) = -B_p \dot{\alpha} \quad (11)$$

The following is the process of linearizing the two nonlinear equations of the rotary inverted pendulum:

Set up  $z^T = [\theta, \alpha, \dot{\theta}, \dot{\alpha}, \ddot{\theta}, \ddot{\alpha}]$  and  $z_0^T = [0, 0, 0, 0, 0, 0]$ , the first nonlinear equation is set as  $f(z)$ :

$$f(z) = \left( m_p L_r^2 + \frac{1}{4} m_p L_p^2 - \frac{1}{4} m_p L_p^2 \cos(\alpha)^2 + J_r \right) \ddot{\theta} - \left( \frac{1}{2} m_p L_p L_r \cos(\alpha) \right) \ddot{\alpha} + \left( \frac{1}{2} m_p L_p^2 \sin(\alpha) \cos(\alpha) \right) \dot{\theta} \dot{\alpha} + \left( \frac{1}{2} m_p L_p L_r \sin(\alpha) \right) \dot{\alpha}^2 \quad (12)$$

The linearization equation is  $f_{lin}(z)$ :

$$f_{lin}(z) = f(z_0) + \left( \frac{\partial f(z)}{\partial \ddot{\theta}} \right) \Big|_{z=z_0} \ddot{\theta} + \left( \frac{\partial f(z)}{\partial \ddot{\alpha}} \right) \Big|_{z=z_0} \ddot{\alpha} + \left( \frac{\partial f(z)}{\partial \dot{\theta}} \right) \Big|_{z=z_0} \dot{\theta} + \left( \frac{\partial f(z)}{\partial \dot{\alpha}} \right) \Big|_{z=z_0} \dot{\alpha} + \left( \frac{\partial f(z)}{\partial \theta} \right) \Big|_{z=z_0} \theta + \left( \frac{\partial f(z)}{\partial \alpha} \right) \Big|_{z=z_0} \alpha \quad (13)$$

Substituting for  $z_0$  can be obtained:

$$(m_p L_r^2 + J_r) \ddot{\theta} - \frac{1}{2} m_p L_p L_r \ddot{\alpha} = \tau - B_r \dot{\theta} \quad (14)$$

In the same way, the linearization of second nonlinear equations can be obtained:

$$- \frac{1}{2} m_p L_p L_r \ddot{\theta} + \left( J_p + \frac{1}{4} m_p L_p^2 \right) \ddot{\alpha} - \frac{1}{2} m_p L_p g \alpha = -B_p \dot{\alpha} \quad (15)$$

Definition  $x = [\theta \ \alpha \ \dot{\theta} \ \dot{\alpha}]^T$   $y = [\theta \ \alpha]^T$   $u = V_m$ , Then the state space equation after linearization is as follows:

$$\begin{aligned}\dot{x} &= Ax + B\mu \\ y &= Cx + D\mu\end{aligned}\quad (16)$$

Substituted the Table1 parameters, we can get the state equation as follows:

$$A = \begin{bmatrix} 0 & 0 & 1 & 0 \\ 0 & 0 & 0 & 1 \\ 0 & 53.1 & -0.6586 & 0.6575 \\ 0 & 98.38 & -0.6575 & 1.218 \end{bmatrix}, B = \begin{bmatrix} 0 \\ 0 \\ 274.4 \\ 274 \end{bmatrix} \quad (17)$$

$$C = \begin{bmatrix} 1 & 0 & 0 & 0 \\ 0 & 1 & 0 & 0 \end{bmatrix}, D = \begin{bmatrix} 0 \\ 0 \end{bmatrix}$$

The transfer function of the rotary arm angle  $\theta$  to the input voltage  $V_m$  :

$$P_1(s) = \frac{274s^2 - 154s - 12446}{s^4 - 0.5594s^3 - 98.7499s^2 - 29.8798s} \quad (18)$$

The transfer function of the pendulum angle  $\alpha$  to the input voltage  $V_m$  :

$$P_2(s) = \frac{274s^2}{s^4 - 0.5594s^3 - 98.7499s^2 - 29.8798s} \quad (19)$$

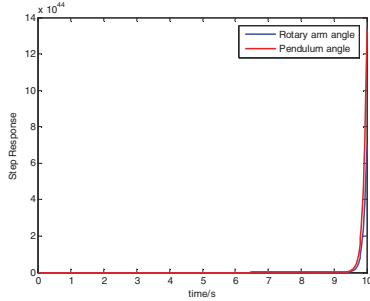


Fig.3 Step response of rotary arm angle and pendulum angle

### 3 Design of fractional order PID controller based on the Bode ideal transfer function

In 1945, in the study of the design of feedback amplifiers, Bode proposed an ideal model of open loop transfer function<sup>[8]</sup>, which is as follows:

$$L(s) = \frac{A}{s^\alpha} = \frac{(\omega_c)^\alpha}{s^\alpha} \quad (0 < \alpha < 2) \quad (20)$$

In which  $\omega_c$  is the cut-off frequency of the system, that is  $|L(j\omega_c)|=1$ , the determination of numerator  $A$  is only related  $\omega_c$ .  $\alpha$  can be an integer or a fraction. In fact, when  $\alpha < 0$ ,  $L(s)$  is a fractional differentiator, and when  $\alpha > 0$ ,  $G(s)$  is a fractional integrator. when  $1 < \alpha < 2$ , The  $L(s)$  amplitude frequency characteristic curve is a slope with a  $-20\alpha dB / dec$  slope, and the phase frequency characteristic curve is a horizontal  $-\alpha\pi / 2$  line. As shown in Fig.4:

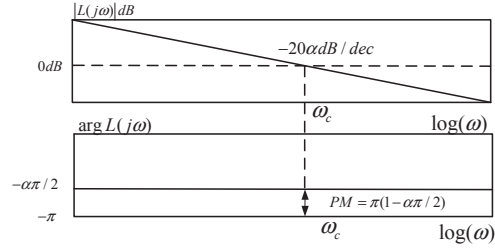


Fig.4 Bode diagram of the Bode ideal transfer function

The Bode ideal transfer function has the following characteristics:

**a. Open-loop characteristics:**

1. A straight line with constant amplitude  $-20\alpha dB / dec$
2. The cut-off frequency  $\omega_c$  depends on the  $A$
3. The phase frequency curve is a  $-\frac{\alpha\pi}{2}$  line
4. The Nyquist curve is a straight line, emitted from the point of origin in the angle of  $-\frac{\alpha\pi}{2}$ .

**b. Closed-loop characteristics:**

1. Gain margin value is  $\infty$  ;
2. Phase frequency margin is  $\phi_m = \pi(1 - \alpha/2)$ , determined by the value of  $\alpha$ .

When  $\omega_c = 1$ ,  $\alpha = 1.2, 1.4, 1.6, 1.8$ ,  $L(s)$  closed-loop step response curve is shown as follows:

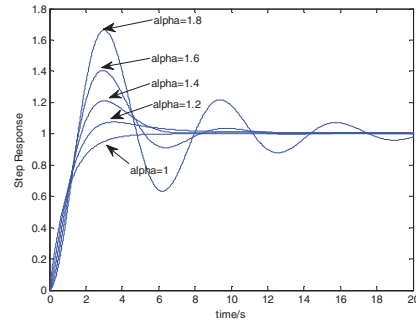


Fig.5 When  $\omega_c = 1$ , the step response curve of the system when  $\alpha$  takes different values

Considering the excellent characteristics of ideal transfer function, we can consider it as a target to design the controller. Because the closed-loop response of Bode ideal transfer function is always stable, make the open-loop transfer function match with the ideal Bode transfer function, and the system will also be corrected to a stable system.

Where,  $G_c$  is the controller,  $G_s$  is the controlled object.

The form of the FOPID controller is as follows:

$$G_c(s) = K_p + \frac{K_i}{s^\lambda} + K_d s^\mu \quad (21)$$

The open-loop transfer function  $T_0(s)$  is:

$$T_0(s) = G_s(s)G_c(s) = G_s(s)(K_p + \frac{K_i}{s^\lambda} + K_d s^\mu) \quad (22)$$

The Bode ideal transfer function  $G_d$  is as follows :

$$G_d(s) = \frac{A}{s^\alpha} \quad 0 < \alpha < 2, \text{ where } A = (\omega_c)^\alpha \quad (23)$$

In the frequency domain, the open-loop transfer function  $T_0(j\omega)$  and the Bode ideal transfer function  $G_d(j\omega)$  match:

$$G_s(j\omega)(K_p + \frac{K_i}{(j\omega)^\lambda} + K_d(j\omega)^\mu) = \frac{A}{(j\omega)^\alpha} \quad (24)$$

The simplified equation is obtained:

$$G_s(j\omega) \left( K_p + K_d \omega^\mu \cos(\mu\pi/2) + \frac{K_i}{\omega^\lambda} \cos(\lambda\pi/2) + i(K_d \omega^\mu \sin(\mu\pi/2) - \frac{K_i}{\omega^\lambda} \sin(\lambda\pi/2)) \right) = \frac{A}{(j\omega)^\alpha} \quad (25)$$

Match the angle of the system at  $\omega_c$  :

$$\phi_0 + \arctan \left( \frac{K_d \omega_c^\mu \sin(\mu\pi/2) - \frac{K_i}{\omega_c^\lambda} \sin(\lambda\pi/2)}{K_p + K_d \omega_c^\mu \cos(\mu\pi/2) + \frac{K_i}{\omega_c^\lambda} \cos(\lambda\pi/2)} \right) = -\frac{\alpha\pi}{2} \quad (26)$$

Among them,  $\phi_0$  is the angle of  $G_s(j\omega_c)$ .

Match the amplitude of the system at  $\omega_c$  :

$$|G_s(j\omega_c)| \sqrt{(K_p + K_d \omega_c^\mu \cos(\mu\pi/2) + \frac{K_i}{\omega_c^\lambda} \cos(\lambda\pi/2))^2 + (K_d \omega_c^\mu \sin(\mu\pi/2) - \frac{K_i}{\omega_c^\lambda} \sin(\lambda\pi/2))^2} = \frac{A}{\omega_c^\alpha} \quad (27)$$

Match the slope of the Nyquist curve at  $\omega_c$ : the slope of the  $T_0(j\omega)$ 's Nyquist curve at  $\omega_c$  is equal to the derivative of  $T_0(j\omega)$  at  $\omega_c$  :

$$\frac{d}{d\omega} T_0(j\omega) = G_s(j\omega) \frac{d}{d\omega} G_c(j\omega) + G_c(j\omega) \frac{d}{d\omega} G_s(j\omega) \quad (28)$$

Because  $\ln G_s(j\omega) = \ln |G_s(j\omega)| + i \angle G_s(j\omega)$

We can get:

$$\frac{d}{d\omega} G_s(j\omega) = G_s(j\omega) \left( \frac{d}{d\omega} \ln |G_s(j\omega)| + i \frac{d}{d\omega} \angle G_s(j\omega) \right) = G_s(j\omega) (L_a + i L_p) \quad (29)$$

Where,

$$\begin{aligned} L_a &= \frac{d}{d\omega} \ln |G_s(j\omega)|, \\ L_p &= \frac{d}{d\omega} \angle G_s(j\omega) \end{aligned} \quad (30)$$

The derivative of the controller  $G_c(j\omega)$  is:

$$\begin{aligned} \frac{d}{d\omega} (G_c(j\omega)) &= \frac{d}{d\omega} (K_p + K_d \omega^\mu (\cos(\mu\pi/2) + i \sin(\mu\pi/2)) + \frac{K_i}{\omega^\lambda} (\cos(\lambda\pi/2) - i \sin(\lambda\pi/2))) \\ &= \mu K_d \omega^{\mu-1} \cos(\mu\pi/2) - \lambda \frac{K_i}{\omega^{\lambda+1}} \cos(\lambda\pi/2) + i(\mu K_d \omega^{\mu-1} \sin(\mu\pi/2) + \lambda \frac{K_i}{\omega^{\lambda+1}} \sin(\lambda\pi/2)) \end{aligned} \quad (31)$$

The derivative of the open-loop transfer function  $T_0(j\omega)$  is:

$$\begin{aligned} \frac{d}{d\omega} T_0(j\omega) &= G_s(j\omega) \left\{ [L_a (K_p + K_d \omega^\mu \cos(\mu\pi/2) + K_i \omega^{-\lambda} \cos(\lambda\pi/2)) - L_p (K_d \omega^\mu \sin(\mu\pi/2) - K_i \omega^{-\lambda} \sin(\lambda\pi/2))] + \right. \\ &\quad \mu K_d \omega^{\mu-1} \cos(\mu\pi/2) - \lambda \frac{K_i}{\omega^{\lambda+1}} \cos(\lambda\pi/2) + i[L_p (K_p + K_i \omega^{-\lambda} \cos(\lambda\pi/2) + K_d \omega^\mu \cos(\mu\pi/2)) + \\ &\quad L_a (K_d \omega^\mu \sin(\mu\pi/2) - K_i \omega^{-\lambda} \sin(\lambda\pi/2)) + K_i \lambda \omega^{-(\lambda+1)} \sin(\lambda\pi/2) + \mu K_d \omega^{\mu-1} \sin(\mu\pi/2)] \} \end{aligned} \quad (32)$$

After finishing, it can be obtained:

$$\phi = \phi_0 + \arctan \left( \frac{D}{N} \right) \quad (33)$$

Among them,  $\phi$  is the angle of the Nyquist curve of the Bode ideal transfer function.

$$\begin{aligned} N &= [L_a (K_p + K_d \omega^\mu \cos(\mu\pi/2) + K_i \omega^{-\lambda} \cos(\lambda\pi/2)) - L_p (K_d \omega^\mu \sin(\mu\pi/2) - K_i \omega^{-\lambda} \sin(\lambda\pi/2)) + \mu K_d \omega^{\mu-1} \cos(\mu\pi/2) - \lambda \frac{K_i}{\omega^{\lambda+1}} \cos(\lambda\pi/2)] \\ D &= [L_p (K_p + K_i \omega^{-\lambda} \cos(\lambda\pi/2) + K_d \omega^\mu \cos(\mu\pi/2)) + L_a (K_d \omega^\mu \sin(\mu\pi/2) - K_i \omega^{-\lambda} \sin(\lambda\pi/2)) + K_i \lambda \omega^{-(\lambda+1)} \sin(\lambda\pi/2) + \mu K_d \omega^{\mu-1} \sin(\mu\pi/2)] \end{aligned}$$

From the above (26), (27), (33) three tuning rules that we can solve the FOPD<sup>[9]</sup> and FOPI<sup>[10]</sup> controller with three parameters, which has five parameters need to add two conditions, because the Bode ideal transfer function of the phase margin has been  $-\frac{\alpha}{2}\pi$ , so we choose  $\omega_b$  and  $\omega_h$

which near  $\omega_c$ , the following two formulas can be obtained:

$$\phi_0 + \arctan \left( \frac{K_d \omega_b^\mu \sin(\mu\pi/2) - \frac{K_i}{\omega_b^\lambda} \sin(\lambda\pi/2)}{K_p + K_d \omega_b^\mu \cos(\mu\pi/2) + \frac{K_i}{\omega_b^\lambda} \cos(\lambda\pi/2)} \right) = -\frac{\alpha\pi}{2} \quad (34)$$

$$\phi_0 + \arctan \left( \frac{K_d \omega_h^\mu \sin(\mu\pi/2) - \frac{K_i}{\omega_h^\lambda} \sin(\lambda\pi/2)}{K_p + K_d \omega_h^\mu \cos(\mu\pi/2) + \frac{K_i}{\omega_h^\lambda} \cos(\lambda\pi/2)} \right) = -\frac{\alpha\pi}{2} \quad (35)$$

With the help of the Fmincon nonlinear optimization function in the optimization toolbox, taking (26) as the objective function, formula (27), (33), (34), and (35) are nonlinear equality constraints, and the parameters can be solved.

#### 4 COMPARISON AND ANALYSIS OF EXPERIMENT RESULTS

Assuming that the pendulum is vertical and upward, the input  $r(s)=0$ , apply a disturbance  $f$  to the system. Therefore, the pendulum angle control structure diagram of the rotary inverted pendulum is as follows:

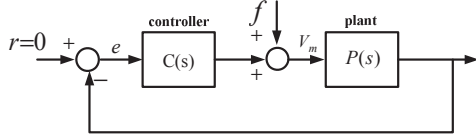


Fig.6 The pendulum angle control structure diagram of the rotary inverted pendulum

Fig.6 can be converted to Fig.7:

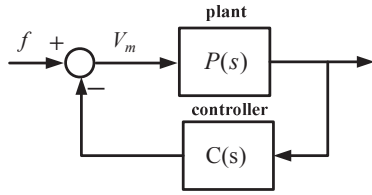


Fig.7 After conversion the pendulum angle control structure diagram. From Fig.7, we can see that this control method only controls one variable, while the output of the rotary inverted pendulum has two variables: the angle of the pendulum and the angle of the rotary arm. so we need two closed-loop control. The rotary inverted pendulum is a dynamic balance, it needs differential adjustment. When the angle change rate is large, the speed of regulation is fast, so differential control is necessary, so the PD control is adopted. Therefore, we first use the two closed-loop IOPD control method to control the angle of the rotary arm and the pendulum angle. Then we use two closed-loop FOPD controller and the two closed-loop FOPID controller for comparative analysis.

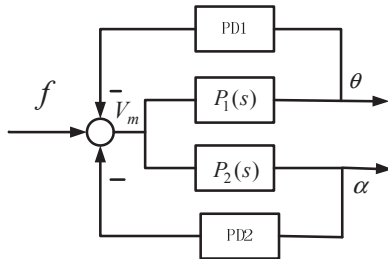


Fig.8 The two closed-loop PD control structure of rotary inverted pendulum

As for IOPD controller, we use the optimpid integer order controller design toolbox<sup>[11]</sup> to solve the controller parameters. For the FOPD、FOPID controller, we choose the Bode ideal transfer function to solve parameters. The Bode ideal transfer function  $L(s)$  we choose is as follows:

$$L(s) = \frac{A}{s^\alpha} = \frac{(\omega_c)^\alpha}{s^\alpha} = \frac{(200)^{5/3}}{s^{5/3}} \quad (36)$$

The Bode diagram of  $L(s)$  is as Fig.9:

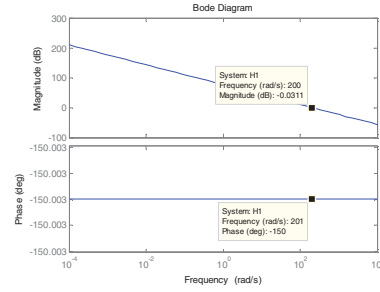


Fig.9 The Bode diagram of  $L(s)$

The two closed-loop IOPD control structure diagram based on the Quanser loop simulation platform is shown as Fig.10:

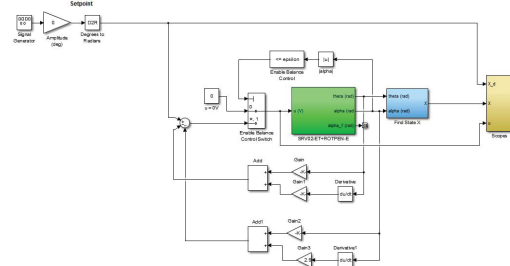


Fig.10 The two closed-loop IOPD control structure diagram

The parameters of IOPD controller are as follows:

$$C_1(s) = K_p + K_d s = -1.75 - 2.2s \quad (37)$$

$$C_2(s) = K_p + K_d s = 23.5 + 2.9s \quad (38)$$

The two closed-loop FOPD control structure diagram based on the Quanser loop simulation platform is shown as Fig.11:

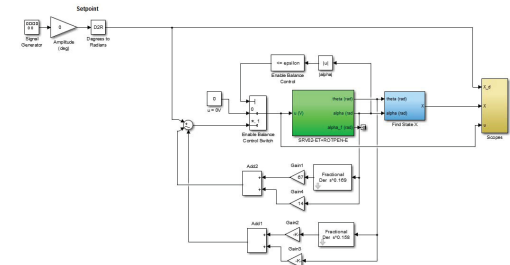


Fig.11 The two closed-loop FOPD control structure diagram

According to FOPD controller parameter tuning rules based on the Bode ideal transfer function<sup>[9]</sup>, the three parameters can be solved:

The parameters of FOPD controller are as follows:

$$C_3(s) = K_p + K_d s^\mu = -0.5 - 68.15s^{0.158} \quad (39)$$

$$C_4(s) = K_p + K_d s^\mu = 14 + 67s^{0.169} \quad (40)$$

The two closed-loop FOPID control structure diagram based on the Quanser loop simulation platform is shown as Fig.12:

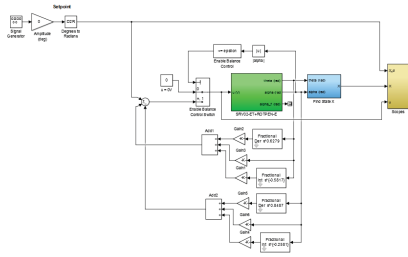


Fig.12 The two closed-loop FOPID control structure diagram

We add two phase angle conditions, the frequency of  $\omega_b$  and  $\omega_h$  we choose is  $\omega_b = 190 \text{ rad/s}$ ,  $\omega_h = 210 \text{ rad/s}$ , according to the five tuning rules, we can get the FOPID controller's parameters are as follows:

$$C_5(s) = K_p + \frac{K_i}{s^\lambda} + K_d s^\mu = -11.011 - \frac{18.966}{s^{0.5817}} - 13.168 s^{0.6279} \quad (41)$$

$$C_6(s) = K_p + \frac{K_i}{s^\lambda} + K_d s^\mu = 20 + \frac{20.277}{s^{0.2582}} + 5.6058 s^{0.8487} \quad (42)$$

The angle response of the rotary arm and the pendulum based on the IOPD, FOPD, FOPID controller is as shown in Fig.13, Fig.14:

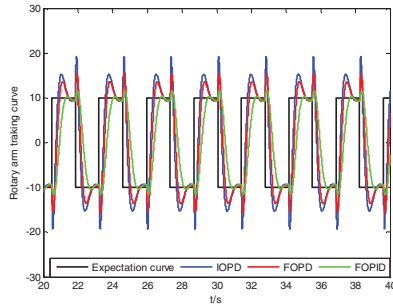


Fig.13 Rotary arm tracking curve based on the IOPD, FOPD, FOPID controller

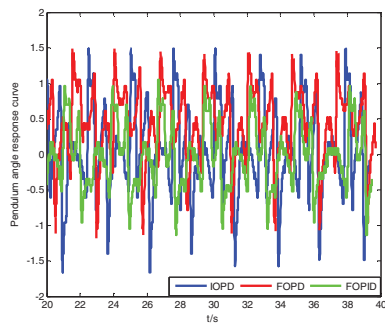


Fig.14 Pendulum angle response curve based on the IOPD, FOPD, FOPID controller

From Fig.13, we can see that the FOPID controller's peak peak angle is 22 degrees, the FOPD controller's peak peak angle is 30 degrees and the IOPD controller's peak peak angle is 38 degrees. The expectation curve's peak peak angle is 20 degrees. We can see that the FOPID controller has the best rotary arm tracking effect.

From Fig.14, we can see that the FOPID controller's peak peak angle is 2 degrees, the FOPD controller's peak peak

angle is 2.7 degrees and the IOPD controller's peak peak angle is 3.2 degrees. The FOPID controller has the best stabilizing pendulum effect, the pendulum is closest to the stable equilibrium point.

## 5 CONCLUSION

This paper presents a method of designing FOPID controller based on Bode ideal transfer function and applies the controller to the rotary inverted pendulum based on Quanser platform. In general, the control effect of the fractional order controller (FOPD, FOPID) is better than the integer order controller (IOPD). In the fractional order controller, the FOPID controller has the best control effect.

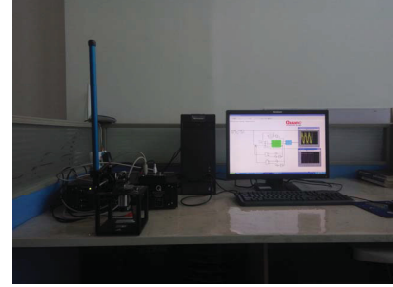


Fig.15 Rotary inverted pendulum experimental device

## Reference

- [1] Reddy N S, Saketh M S, Pal P, et al. Optimal PID controller design of an inverted pendulum dynamics: A hybrid pole-placement & firefly algorithm approach[C]// IEEE First International Conference on Control, Measurement and Instrumentation. IEEE, 2016:305-310.
- [2] Hernández-Guzmán V M, Antonio-Cruz M, et al. Linear State Feedback Regulation of a Furuta Pendulum: Design Based on Differential Flatness and Root Locus[J].IEEE Access, 2017, 4(99):8721-8736.
- [3] Chen C, Zhao Y, Gao J F. Comparative analysis of PID and LQR control algorithms based on a single inverted pendulum [J]. Value engineering, 2015 (18): 209-210.
- [4] Huang Y H, Zhang L, Zhang P P. Fuzzy Control Research on single stage inverted pendulum [J]. Automation of manufacturing industry, 2015 (1): 1-3.
- [5] Chen Y Q, Dou H, Vinagre B M, et al. A robust tuning method for fractional order PI controllers [J]. IFAC Proceedings Volumes, 2006, 39(11):22-27.
- [6] Quanser Inc.SRV02 Rotary Pendulum User Manual,2010
- [7] Quanser Inc. Rotary Pendulum Workbook.
- [8] C.A.Monje,B.M.Vinagre,V.Feliu,Y.Chen,andD.Xue,"Fractional Order systems and controls fundamentals and applications,"Springer,2010
- [9] Bhisikar K K, Vyawahare V A, Joshi M M. Design of fractional order PD Controller for Unstable and Integrating Systems[C]// Intelligent Control and Automation. IEEE, 2015:4698-4703.
- [10] Bhisikar K K, Vyawahare V A, Tare A V. Design of Fractional order PI controller for linear unstable systems[C]// IEEE Students' Conference on Electrical, Electronics and Computer Science. IEEE, 2014:1-6.
- [11] Xue D Y. Control system computer and design --MATLAB language and application [M]. Tsinghua University press, 1996.